INTERNATIONAL JOURNAL OF CLIMATOLOGY
Int. J. Climatol. (2013)
Published online in Wiley Online Library
(wileyonlinelibrary.com) DOI: 10.1002/joc.3650

RMetS
Royal Meteorological Society

Climate change projections of precipitation and reference evapotranspiration for the Middle East and Northern Africa until 2050

Wilco Terink,* Walter Willem Immerzeel and Peter Droogers
FutureWater, Wageningen, The Netherlands

ABSTRACT: The Middle East and North Africa (MENA) region can be considered as the most water-scarce region of the world. The Intergovernmental Panel on Climate Change projects strong changes in climate across MENA, further exacerbating pressure on available water resources. The objective of this study is to undertake a climate change assessment for 22 MENA countries in order to quantify the problems these countries may encounter up to 2050. To evaluate climate change in MENA, nine global circulation models representing two future periods (2020–2030 and 2040–2050) were statistically downscaled and compared with a current climate, defined as the period 2000–2009. Besides precipitation only this study also focuses on change in water demand by vegetation reference evapotranspiration (ETref). It was found that for both future periods the annual precipitation sum will decrease for the majority of countries, with decreases of 15–20% for the latter period. For some countries, e.g. Djibouti and Yemen, an increase in annual precipitation of 15–20% was found. The annual ETref shows an increase for all countries for both future periods, with the strongest increases for the latter period. For the extreme situation, it was found that the minimum monthly and annual precipitation sum does not become smaller in the future climate. It in fact increases. In contrast, the maximum monthly and annual ETref increases for all countries. This indicates that projected changes in demand are likely to have a more adverse effect than changes in supply. Spatial analysis showed that the largest precipitation decreases are to be found in southern Egypt, Morocco, central and coastal Algeria, Tunisia, central Libya, Syria, and central and eastern Iran. A case study for Morocco revealed that the potential water deficit, which is already apparent for the current climate, becomes even larger for the future climate.
Copyright © 2013 Royal Meteorological Society

KEY WORDS MENA; Africa; Middle East; climate change; precipitation; reference evapotranspiration; GCM; downscaling

Received 14 May 2012; Accepted 17 December 2012

1. Introduction

The Middle East and Northern Africa (MENA) region can be considered as the most water-scarce region of the world. Large-scale water management problems are already apparent in the region. Aquifers are overpumped, water quality is deteriorating, and water supply and irrigation services are often rationed – with consequences for human health, agricultural productivity, and the environment. According to Roudi-Fahimi and Kent (2007), the MENA region's population stood at 432 million in 2007, and is projected to reach nearly 700 million by 2050. This alone would lead to a fall in per capita water availability by almost 40% by 2050. Moreover, climate change will affect weather and precipitation patterns with the consequence that the MENA region may see more frequent and severe droughts. The Fourth Assessment Report of the Intergovernmental Panel on Climate Change (IPCC) (IPCC, 2007) projects strong changes in climate across the MENA region. Temperature increases combined with substantial decreases in precipitation are projected. An increase in temperature results in a higher evapotranspiration demand and will, in combination with a decrease in precipitation, severely stress the water resources in the region. According to Christensen *et al.* (2007), regional projections in Africa can be summarized as follows: (1) all of Africa is likely to warm during the 21st century, (2) warming is very likely to be larger than the global, annual mean warming throughout the continent and in all seasons, with drier subtropical regions warming more than the moister tropics, (3) annual rainfall is likely to decrease in much of Mediterranean Africa and northern Sahara, and (4) there is likely to be an increase in annual rainfall in East Africa. As stressed by the IPCC (2007) and Christensen *et al.* (2007), it is clear that the available water resources in the MENA region will be altered owing to the effects of climate change. However, these studies, amongst many other ones, have a rather specific focus and do not cover important aspects relevant for further research and decision making. These shortcomings can be summarized as follows: (1) focus on the continental or regional scale (e.g. Giorgi and Francisco, 2000a; Christensen *et al.*, 2007) rather than

* Correspondence to: W. Terink, FutureWater, Costerweg 1V, 6702 AA Wageningen, The Netherlands. E-mail: w.terink@futurewater.nl

Copyright © 2013 Royal Meteorological Society

on country (or sub-country) scale, (2) analysis based on annual totals (e.g. Arnell *et al.*, 2003) rather than on seasonal and/or monthly values, (3) focus on water supply (rainfall) and warming (temperature) (e.g. Paeth and Hense, 2004; Anyah and Semazzi, 2007; Immerzeel, 2008; Shongwe *et al.*, 2009, 2011; Hurkmans *et al.*, 2010; Terink *et al.*, 2010) rather than on combined supply and demand change (evapotranspiration), and finally (4) single global circulation model (GCM) selection (e.g. Zwiers and Kharin, 1997; Giorgi and Francisco, 2000b; Anyah and Semazzi, 2007; Hurkmans *et al.*, 2010) instead of using multiple GCMs. For the MENA region, there is a strong need for a complete picture of the impact of climate change taking into account these four aspects.

The overall objective of this study is to undertake a climate change assessment for the MENA countries by analysing the change in precipitation and reference evapotranspiration (ETref) in order to stress the water-related problems these countries may encounter around 2050.

Although the IPCC report provides a good indication for possible magnitude of climate change, there are some inherent shortcomings related to the continental scale of the analysis that we attempt to overcome in this study. Therefore, this study is unique in its approach because (1) we use an ensemble of nine GCMs and statistically downscale the model outputs using a high-resolution reference dataset, (2) we focus on the combined supply (precipitation) and demand (ETref) change instead of only on the demand and warming (temperature), (3) we assess intra-annual change in precipitation and ETref with the aim to identify critical periods with regard to water availability, and (4) we aggregate and present results at the country level, which is the appropriate scale for interventions.

The results of this approach are very valuable for a range of other applications from impact and adaptation assessment to water planners. A demonstration of this approach from this specific case is presented in Immerzeel *et al.* (2012) and Droogers *et al.* (2012). The first study will evaluate the water availability in the MENA region around 2050 using the PCRGLOB-WB hydrological model (van Beek and Bierkens, 2009). The second study will focus on the water supply to meet the growing water need, the various options to meet this need, and associated marginal cost of water supply.

2. Study area, data, and methodology

2.1. Study area

The MENA region (Figure 1) with 22 countries is located in the middle east and northern part of Africa. It is an economically diverse region that includes both oil-rich countries in the Gulf and countries that are resource scarce in relation to population, such as Egypt, Morocco, and Yemen. The region is diverse in its landscapes and climates, from the snowy peaks of the Atlas Mountains to the empty quarter of the Arabian Peninsula. The MENA region can be classified according to the aridity index, which is defined as the ratio between precipitation and ETref. On the basis of this index, the largest part of MENA can be classified as hyper-arid (<0.05) (World Bank, 2007). This hyper-arid area includes the inland in Northern Africa (Algeria, Libya, and Egypt). The coastal areas of Northern Africa, Iran, and the Western coastal region of the Middle East are defined as arid to semi-arid. Humid areas are found in the northern parts of Morocco, Algeria, Tunisia, Iraq, and Iran, and the western part of Syria and Lebanon.

Population densities in MENA are largest in semi-arid to humid regions, or where irrigation systems are present. Irrigation systems are mainly concentrated in the Nile Delta in Egypt, where it covers 60–80% of the surface area (World Bank, 2007), in the central part of Iraq, and scattered throughout Iran. Despite the presence of some humid regions and irrigation systems, the MENA region faces many challenges.

The largest challenge in the MENA region is that countries have to manage an unusual combination of a low annual precipitation that is at the same time highly variable. Three groups of countries can be identified:

1 Countries that on average have adequate quantities of renewable water, but the within-country and within-year variations are problematically large. These include Djibouti, Iran, Lebanon, Morocco, Tunisia, and the West Bank.
2 Countries with consistently low levels of renewable water resources. Therefore, these countries are highly dependent on non-renewable groundwater sources and supplies by desalination of sea water. These countries include Bahrain, Gaza, Jordan, Kuwait, Libya, Oman, Qatar, Saudi Arabia, the United Arab Emirates, and Yemen.
3 Countries that mainly dependent on the inflow of transboundary rivers such as the Nile, the Tigris, and the Euphrates. These countries include Syria, Iraq, and Egypt (World Bank, 2007).

Because the MENA region is the most water-scarce region of the world, good water management is essential. According to World Bank (2007), most of the MENA region's countries cannot meet their current water demand, and the situation is to get worse because of climate change and population increase.

2.2. Data

This study compares a current climate, which is defined as the period 2000–2009, with two future climate periods: 2020–2030 and 2040–2050. Climate change in the MENA region is evaluated using the A1B GHG emission scenario, which is a scenario of one of the four IPCC scenario families (A1, A2, B1, and B2) (SRES, 2000). This scenario was chosen because it is the most likely scenario; it assumes a world of rapid economic growth, a global population that peaks in mid-century, and a

Copyright © 2013 Royal Meteorological Society

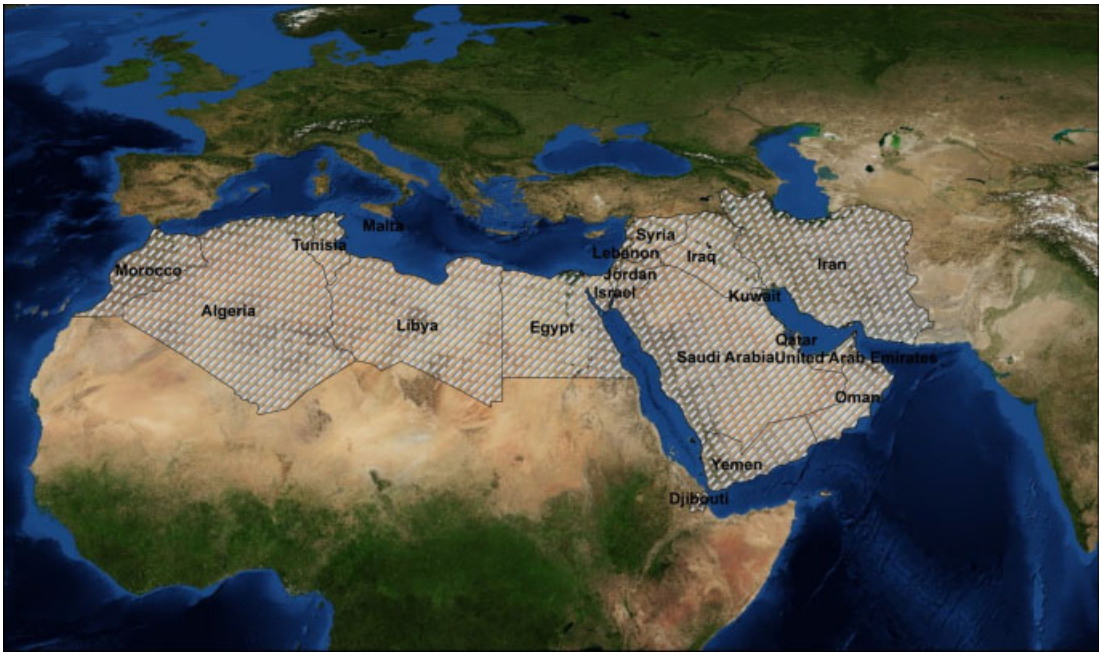

Figure 1. Spatial domain of the Middle East and North African (MENA) countries. The MENA countries (22 in total) are shaded. This figure is available in colour online at wileyonlinelibrary.com/journal/joc

rapid introduction of new and more efficient technologies (IPCC, 2007). The A1B scenario assumes a balance across all sources, which is defined as not relying too heavily on one particular energy source, where the energy sources are defined as not fossil-intensive and non-fossil. Currently, new emission scenarios (CMIP5 multi-model ensemble) (Hibbard *et al.*, 2007; Meehl and Hibbard, 2007; Meehl *et al.*, 2009; WCRP, 2011; Taylor *et al.*, 2012) are available. The focus of this study is exclusively on climate data from the CMIP3 model ensemble because it includes the full bandwidth of possible future climates. The complete CMIP5 model ensemble was unavailable at the time of the study and this would introduce a possible bias in our results. Moreover, the new approach adopted for AR5 based on representative concentration pathways (RCPs) is just a slight improvement from the SRES approach used for AR4. A systematic comparison between CMIP3 and CMIP5 models and the SRES and RCP approaches would however definitely be recommendable for a future study.

Instead of using only one GCM, which is done in many other studies (e.g. Zwiers and Kharin, 1997; Giorgi and Francisco, 2000b; Anyah and Semazzi, 2007; Hurkmans *et al.*, 2010), this study uses forcing data of a current climate and nine GCMs to evaluate climate change for each of the 22 MENA countries. Shongwe *et al.* (2009, 2011) evaluated the performance of all IPCC GCMs in different regions of Africa by comparing their precipitation outputs from 1960 to 1990 with the CRU TS2.1 dataset (New *et al.*, 2000). CRU TS2.1 provides gridded values of observed monthly climate data. Results for Northeast Africa are shown in Table I, and are based on the mean of monthly correlation and root-mean-squared error (RMSE) between the 20th century GCM experiments and the CRU TS2.1 analysis. The best nine performing GCMs were selected to be used in this study. The WCRP CMIP3 multi-model database (http://esg.llnl.gov:8080/index.jsp) provided the monthly climate data of the nine selected GCMs, available for 2000–2050. This database was only used to retrieve the transient monthly GCM temperature data from 2000 to 2050. The IPCC Data Distribution Centre (http://www.ipcc-data.org/) provided the monthly precipitation anomalies between 1961–1990 and 2046–2065. For precipitation these anomalies were used because the statistical downscaling method differs as outlined in Section 2.3..

For the current climate, the Tropical Rainfall Measuring Mission (TRMM, http://trmm.gsfc.nasa.gov/; Kummerow *et al.*, 2000) 3B42 daily product was used for precipitation. TRMM is the only satellite with an active precipitation radar onboard and is available at a spatial resolution of 0.25 km (~25 km), its spatial extend covers the entire MENA region, and it covers the entire time span from January 2000 through December 2009. TRMM data were made available by the Goddard Earth Sciences Data and Information Services Centre of NASA (National Aeronautics and Space Administration).

The ETref of the current climate was calculated using the method of Hargreaves (Hargreaves and Samini, 1985; Droogers and Allen, 2002):

$$\mathrm{ETref}_i = 0.0023 \times 0.408 \times \mathrm{Ra} \times \left(T_{\mathrm{avg}}i + 17.8\right) \times \left(T_{\max}i - T_{\min}i\right)^{0.5}$$

where ETref_i is the reference evapotranspiration on day i, Ra is the extraterrestrial radiation expressed in ($\mathrm{MJ\,m^{-2}\,d^{-1}}$), $T_{\mathrm{avg}}i$ is the average daily temperature (°C), $T_{\max}i$ is the maximum daily temperature (°C), and

Copyright © 2013 Royal Meteorological Society

Table I. Overview of GCM performance in Northeast Africa.

Model	r	RMSE ($mm\,d^{-1}$)	Included
BCCR CM2.0	0.81	1.12	1
CCCMA CGCM 3.1T47	0.79	1.12	1
CNRM CM3	0.79	1.23	1
CSIRO Mk3.0	0.75	0.97	1
GFDL CM2.0	0.82	1.00	1
IPSL CM4	0.78	0.84	1
MPI ECHAM5	0.88	0.59	1
HadCM3	0.76	0.90	1
HadGEM1	0.81	0.78	1
CCCMA CGCM 3.2T63	0.84	1.22	0
GFDL CM2.1	0.68	1.03	0
GISS AOM	0.59	1.60	0
GISS EH	0.65	1.19	0
GISS ER	0.71	1.18	0
IAP FGOALS 1.0g	0.60	1.19	0
INM CM3.0	0.58	1.07	0
MIROC 3.2 (hi-res)	0.83	1.59	0
MIROC 3.2 (med-res)	0.76	1.17	0
MIUB ECHO-G	0.61	1.56	0
MRI CGCM 2.3.2a	0.81	1.78	0
NCAR CCSM 3	0.54	1.79	0
NCAR PCM1	0.55	2.11	0

The first nine GCMs are included in this study. The precipitation mean of monthly correlation and the root-mean-squared error of the 20th century GCM experiments with the CRU TS2.1 analysis are shown (Shongwe *et al.*, 2009, 2011).

$T_{\min}i$ is the minimum daily temperature (°C). This is a well-known method for the calculation of ETref, if only average temperature, maximum temperature, and minimum temperature are available. The Penman–Monteith equation (Allen and Pereira, 1998) is in principle a more accurate method for estimating the ETref as this method is based on more physical approaches, but it needs more input parameters such as the net radiation, soil heat flux, and vapour pressure deficit of the air, which were not available for the required spatial and temporal resolution. It has been demonstrated that if these data were not accurately available at these resolutions, the Hargreaves method might outperform the Penman–Monteith equation (Droogers and Allen, 2002). To derive the ETref for the current climate, NCEP/NCAR Reanalysis 1 (NCEP-1) surface fluxes (Kalnay *et al.*, 1996) were used. The NCEP/NCAR Reanalysis 1 project uses a state-of-the-art analysis/forecast system to perform data assimilation using past data from 1948 to the present. NCEP-1 is known to have systematic errors in the period before 1980, but this does not affect the results in this study because we only use NCEP-1 data from the period 2000–2050. This dataset was used for several reasons: (1) its available spatial resolution is 1.9°, which was the smallest resolution available for average, maximum, and minimum temperatures for the desired period of time and period of interest, (2) it has a daily temporal resolution, and (3) it covers the period from January 2000 through December 2009. These data were made available by the Earth System Research Laboratory of the National Oceanic and Atmospheric Administration.

2.3. Statistical downscaling

The output of GCMs cannot be used directly in this study for three different reasons: (1) the resolution of GCMs is too large [typically of the order 50 000 km^2 (Wilby *et al.*, 2002)], which is too coarse for detailed hydrological assessments, (2) the time series for the past climate, which can also be generated by GCMs, shows a statistically different pattern than the observed climate records, and (3) the size of some countries is very small and therefore they are only covered within one GCM grid cell. This has led to the development of downscaling methodologies. The field of downscaling is divided into two approaches (Haylock *et al.*, 2006): the nesting of high-resolution regional climate models (RCMs) in the GCMs [dynamical downscaling (Giorgi and Mearns, 1991)] and the statistical representation of desired fields from the coarse-resolution GCM data [statistical downscaling (Haylock *et al.*, 2006)]. Several studies have reviewed statistical downscaling methodologies (Giorgi and Mearns, 1991; Hewitson and Crane, 1996; Wilby and Wigley, 1997; Wilby *et al.*, 1998). While in the long term RCMs hold the greatest promise for regional-scale analysis, this approach is still in development, requires detailed surface climate data, and is dependent on high-end computer availability (Hewitson and Crane, 1996).

This study uses a statistical downscaling method because multiple GCMs are used, which would require enormous high-end computer availability if a dynamical downscaling method would be used. Also, detailed surface climate data would be needed, which is not available for the MENA countries. Moreover, it has been proven that a statistical downscaling method has similar performance as a dynamical downscaling approach. For example, Wilby *et al.* (2000) applied downscaled precipitation from both a dynamical downscale model and a statistical downscale model to a hydrological model, and compared the daily precipitation, runoff, and temperature with observations in the Animas River basin, Colorado. A comparable performance was found for the statistical downscaling model and output from an RCM. Also, Murphy (1999) found that a linear regression statistical model had comparable skills to an RCM in downscaling monthly precipitation and temperature at 976 European stations. Another study (Kidson and Thompson, 1998) found that a statistical method, using a regression technique, and a dynamical method showed similar results when they downscaled daily precipitation and minimum and maximum temperatures in New Zealand.

The forcing data of the current climate and nine selected GCMs are distributed at different spatial resolutions. These resolutions need to be uniform for comparison reasons, and to force eventually the PCRGLOB-WB model (Immerzeel *et al.*, 2012), which runs at a spatial resolution of 10 km. First of all, the current climate data (TRMM precipitation and NCEP/NCAR temperature fields) were spatially downscaled to a resolution of 10 km in Africa Albers Equal-Area projection (Snyder, 1987), using spline interpolation (Mitasova and Mitas, 1993). This method uses a mathematical function that

Copyright © 2013 Royal Meteorological Society

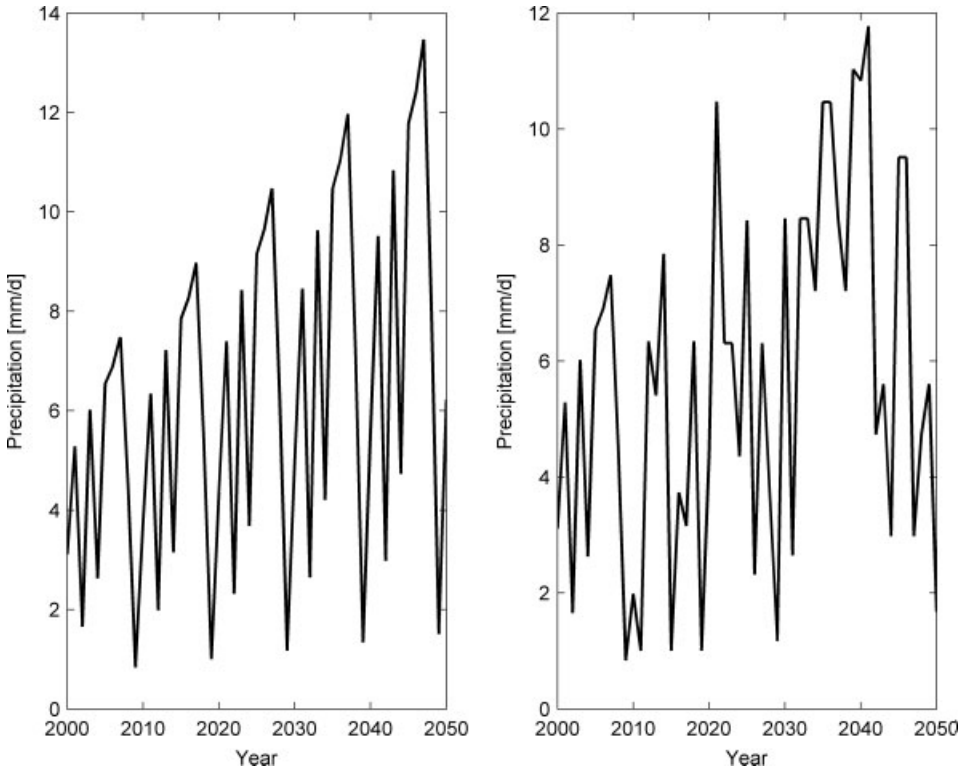

Figure 2. Example of downscaling climate change scenarios using a non-random approach (left) and a random approach (right) as applied in this study.

minimizes overall surface curvature, resulting in a smooth surface that passes exactly through the input points. The ETref of the current climate is subsequently calculated using the projected and downscaled daily average, minimum, and maximum temperatures, using the Hargreaves method as shown before. Second, the future climate forcing data (2010–2050) of the nine selected GCMs were statistically downscaled to the same spatial resolution and daily time step as the current period. The statistical downscaling approach is slightly different for the ETref and precipitation, as outlined hereafter.

First of all, a future temperature dataset for each GCM was created, which is required for the calculation of the ETref. The future temperature data for each GCM were statistically downscaled as follows:

1. A time series with random years was created, based on the years 2000–2009. This means that for each year in the period 2010–2050, a random year was selected from the period 2000–2009. Selecting random years is necessary to produce a natural transient daily time series of future climate data. If we would repeat the current climate over the entire period, then the time series would show an unrealistic recurrence interval of 10 years (Figure 2).
2. For each GCM, the average temperature per month was calculated for the current period 2000–2009.
3. For each month in 2010–2050, the absolute difference in temperature with respect to the average value (result from step 2) was calculated.
4. The temperature differences from step 3 were projected to Africa Albers Equal-Area projection, and spatially downscaled to 10 km, using spline interpolation (Mitasova and Mitas, 1993).
5. For each day in 2010–2050, the future temperature is calculated using:

$$\mathrm{TF}_i = \mathrm{TR}_i + \Delta T_{y,m}$$

where TF_i is the future temperature (°C) on day i (1–365), TR_i is the temperature (°C) in the random year on day i (1–365), and $T_{y,m}$ is the temperature difference (°C) for year y (2010–2050) during month m (1–12).
6. Finally, the future ETref for each GCM is calculated with Hargreaves (Hargreaves and Samini, 1985), using the statistically downscaled temperature (step 5), and the minimum and maximum temperatures from the specific day of the random year.

For precipitation a different procedure was chosen, because for precipitation a change factor is required instead of an absolute difference in precipitation. In the MENA region there are extensive areas where monthly precipitation is close to zero. If we would calculate the anomaly (factor) between the monthly precipitation and the average precipitation for that month during 2000–2009, then it may happen that we divide by a very small (almost zero) value, resulting in erroneous large precipitation factors. If this would be interpolated to a resolution of 10 km, then large areas could be

Copyright © 2013 Royal Meteorological Society

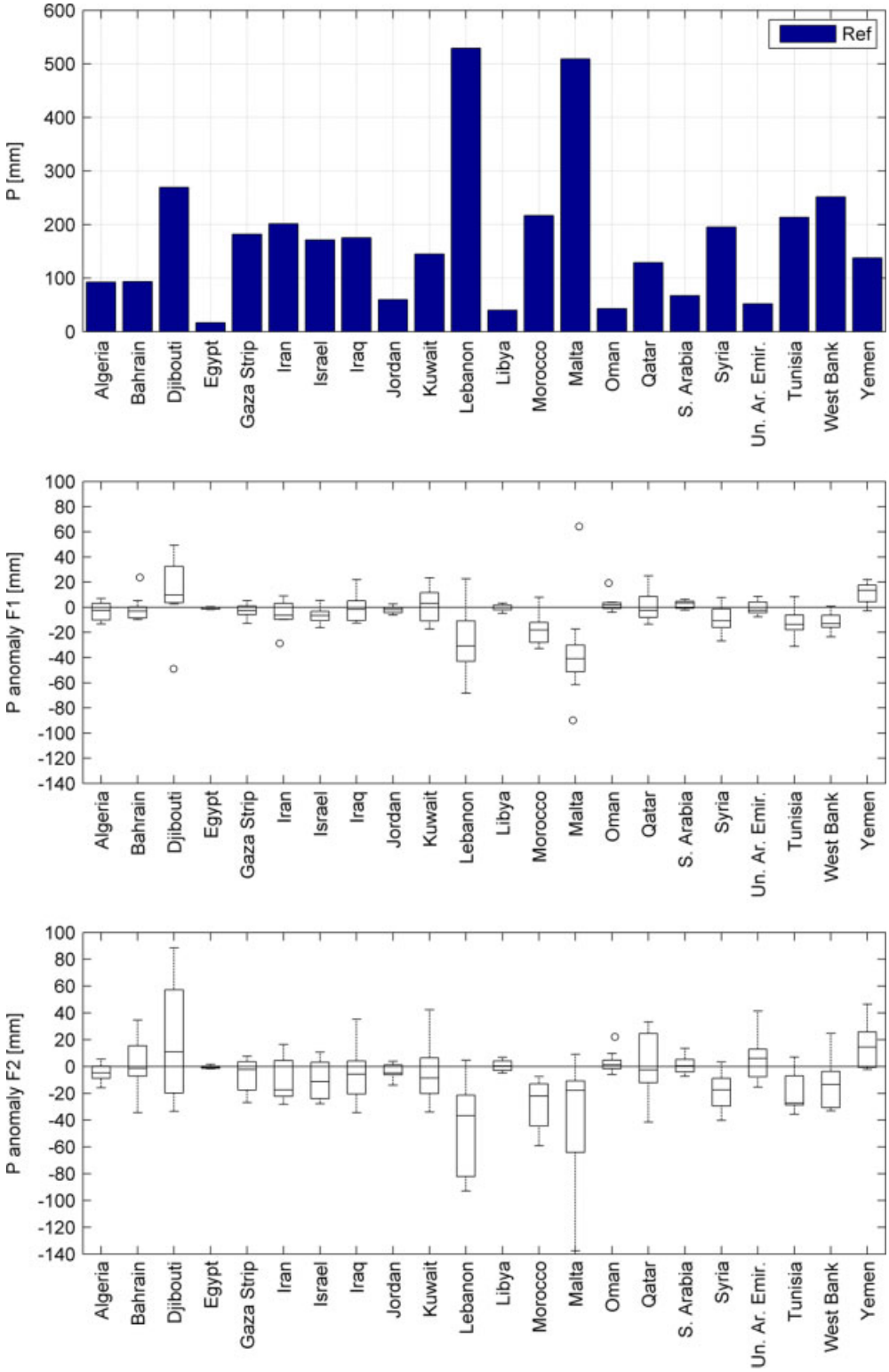

Figure 3. Top: Average annual precipitation sum of the current climate for each of the 22 MENA countries. Middle: Boxplot of average annual precipitation anomaly of F1 (2020–2030) with respect to the current climate. The box shows the range between the GCMs. Bottom: Same as middle, but for F2 (2040–2050). This figure is available in colour online at wileyonlinelibrary.com/journal/joc

affected by these large factors. This means that in areas where precipitation should decrease in the future, it could instead increase because of the interpolation of these large factors. To statistically downscale the future precipitation data, the following steps were taken:

1. A time series with random years was created, as was done for temperature.
2. The monthly precipitation anomalies and monthly reference precipitation of 1961–1990 were projected to the Africa Albers Equal-Area projection, and

Copyright © 2013 Royal Meteorological Society

spatially downscaled to 10 km, using spline interpolation.

3. Consecutively, for each month (1–12), a correction factor for that month was calculated by dividing the anomalies by the reference precipitation for that month. This factor, however, is representative for the anomaly from 1961–1990 to 2046–2065, which is a period of approximately 80 years in length. An annual correction factor was determined assuming that the change for precipitation occurs linearly in time.
4. Finally, the future precipitation for each GCM is calculated using:

$$PF_i = PR_i + (PR_i \times (y - 2009) \times Pfac_m)$$

where PF_i is the future precipitation (mm) on day i (1–365), PR_i is the precipitation in a random year on day i (1–365), y is a future year (2010–2050), and $Pfac_m$ is the precipitation factor in month m (1–12).

3. Results

3.1. Average annual precipitation

The annual change in precipitation for each of the 22 MENA countries has been analysed in Figure 3. Figure 3 (top) shows the average annual precipitation sum for the current climate (2000–2009) for each of the 22 MENA countries. The middle of Figure 3 shows the anomalies of F1 (2020–2030), whereas the anomalies of F2 (2040–2050) are shown in the bottom of Figure 3. The anomalies in these boxplots show the range between the GCMs. On the basis of these results, it is clear that most countries will experience a decrease in precipitation for F1 and F2, with the largest decreases found for F2. Some countries, however, e.g. Yemen and Djibouti, are projected to have an increase in annual presentation. Yemen appears to receive 15 mm (11%) more precipitation for F1 and F2, and Djibouti 10 mm (4%) more precipitation for both F1 and F2. This is a very positive development for Yemen because the country is already low on precipitation (140 mm annual). Countries with the largest decrease in precipitation are Lebanon, Morocco, and Malta. Considering the median of GCMs, this decrease is for F1 30 mm (6%) for Lebanon, 18 mm (8%) for Morocco, and 40 mm (8%) for Malta. Decreases for F2 are in the order of 38 mm (7%) for Lebanon, 20 mm (9%) for Morocco, and 20 mm (4%) for Malta. Climate predictions for the far future are more uncertain than climate predictions for the near future. This uncertainty is reflected in the range between the GCMs, which is larger for F2 than for F1. If we consider the 25th percentile of GCMs of F2, then we notice a decrease of 45 mm (20%) for Morocco, 80 mm (16%) for Lebanon, and 65 mm (13%) for Malta. Morocco will become very vulnerable to climate change in the future, because currently Morocco already has a low annual precipitation sum, which will become even smaller based on these projections. Also, Algeria has a low annual precipitation sum (90 mm) for the current climate. With a decrease of 10 mm (11%) for both F1 and F2, Algeria is also vulnerable to climate change. It is interesting that for some countries, the range in GCM predictions is relatively small, e.g. for Egypt, Jordan, Libya, and Oman. This means that the uncertainty in climate predictions is considerably smaller for these countries. Egypt, being the country with the smallest annual precipitation sum, can expect hardly any change in precipitation. Besides this, Egypt is also fed by the river Nile, meaning that this country is less depending on precipitation within the country.

3.2. Average annual ETref

Many climate impact studies only focus on the change in precipitation and temperature, instead of including the change in ETref as well (e.g. Paeth and Hense, 2004; Anyah and Semazzi, 2007; Immerzeel, 2008; Shongwe *et al.*, 2009, 2011; Hurkmans *et al.*, 2010; Terink *et al.*, 2010). It is far more relevant to focus on the change in ETref in combination with the change in precipitation, because this gives an indication of possible changes in water stress. Figure 4 (top) represents the average annual ETref for the current climate for each of the 22 MENA countries. Again, the boxplots show the range in anomalies between the nine selected GCMs. The majority of countries can expect an increase in ETref for both F1 and F2, except for Egypt, Iraq, Jordan, Libya, Malta, and Syria, which show a decrease in ETref for F1. The increase in ETref is most significant for F2. An increase in ETref can be translated into an increased demand for water. Moreover, higher ETref will enhance the actual water transpired by the natural vegetation decreasing groundwater recharge and runoff to surface water even more. Morocco and Algeria appear to show an increase in ETref and a decrease in precipitation for both future periods, meaning that water stress will become an even more severe problem in these countries in the future. Jordan and Syria, being countries with a low annual precipitation sum for the current climate, both show a decrease in precipitation for F1 and F2. A point of attention is that both countries show a decrease in ETref for F1, and an increase in ETref for F2.

3.3. Annual extremes

The change in climate extremes has been evaluated by analysing the change in minimum annual precipitation and maximum annual ETref. This combination provides an outlook of how the water shortage may change in the future for the extreme situation. The minimum annual precipitation for the current climate is shown in the top of Figure 5. The anomalies of F1 are shown in the middle of Figure 5, and the anomalies of F2 are shown in the bottom of Figure 5. These boxplots show the range in anomalies between the GCMs. The same is done in Figure 6, but for the maximum annual ETref. Despite the fact that the average annual precipitation decreases for most countries, as was shown in Figure 3, there is no significant decrease

Copyright © 2013 Royal Meteorological Society

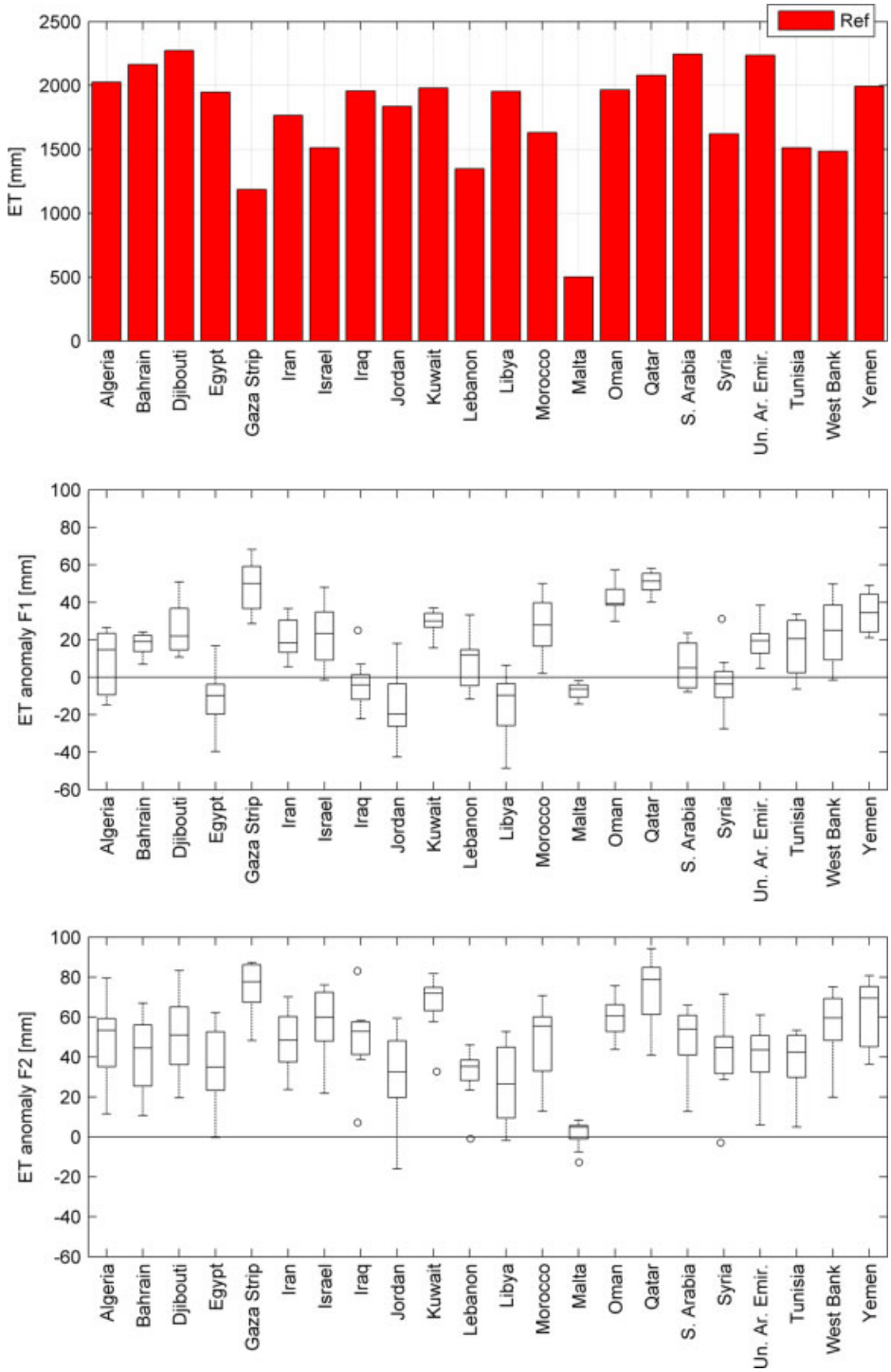

Figure 4. Top: Average annual reference evapotranspiration (ETref) of the current climate for each of the 22 MENA countries. Middle: Boxplot of average annual ETref anomaly of F1 (2020–2030) with respect to the current climate. The box shows the range between the GCMs. Bottom: Same as middle, but for F2 (2040–2050). This figure is available in colour online at wileyonlinelibrary.com/journal/joc

in minimum annual precipitation. For F1, the majority of GCMs in fact projects an increase in minimum annual precipitation. For F2, the range in GCM projections is larger with more GCMs projecting an increase in minimum annual precipitation. Although the extremes in low precipitation do not become more extreme in the future, the maximum annual ETref (Figure 6) appears to increase in the future. This is particularly true for F2, where all GCMs (except for Malta and Tunesia) project an increase in annual maximum ETref.

3.4. Monthly analysis

To evaluate the water availability throughout the year, the monthly change in precipitation and ETref is very relevant. To evaluate this we have taken two steps: first we have calculated the statistics (average, min, and max)

Copyright © 2013 Royal Meteorological Society

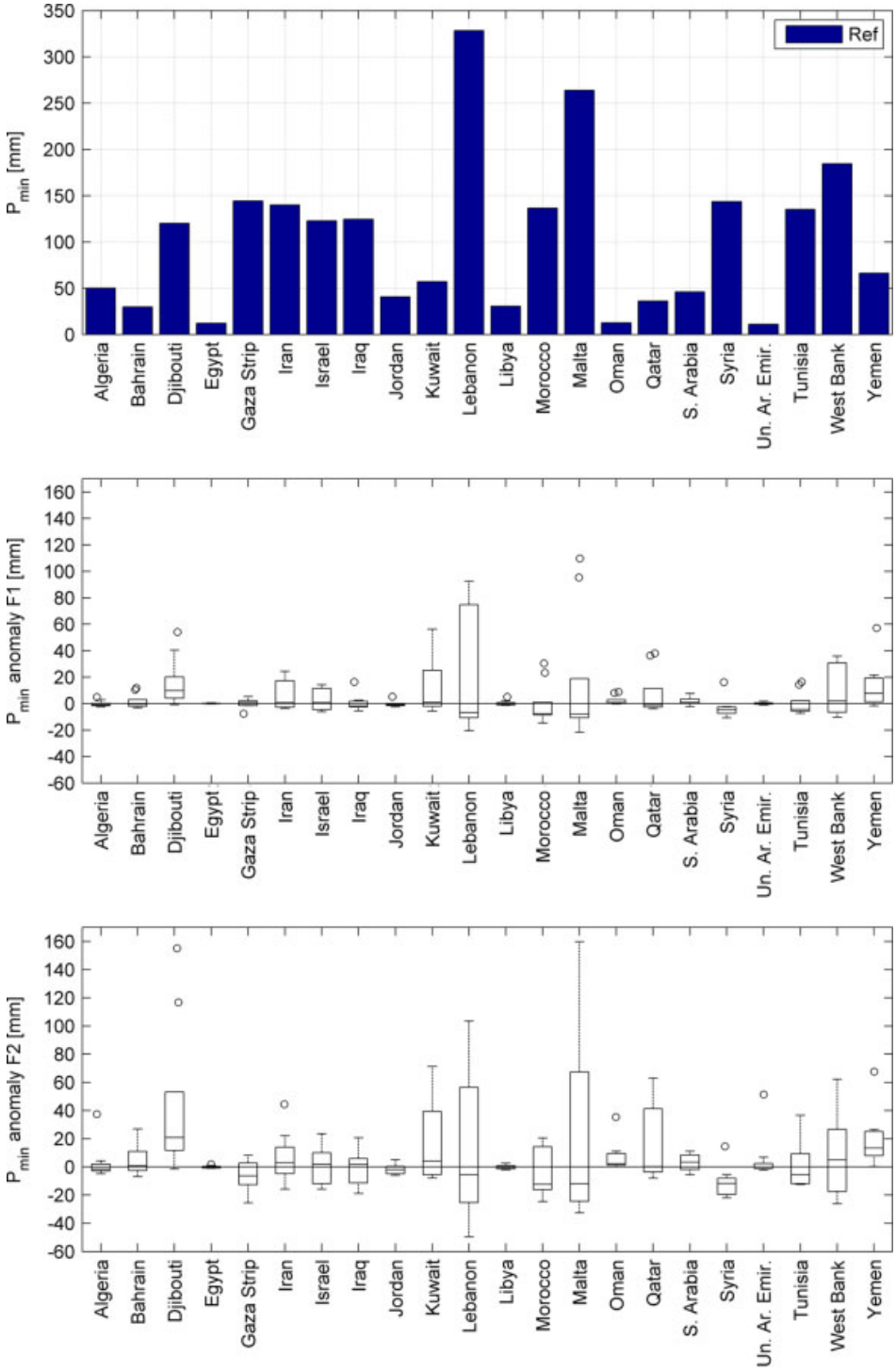

Figure 5. Top: Minimum annual precipitation of the current climate for each of the 22 MENA countries. Middle: Boxplot of minimum annual precipitation anomaly of F1 with respect to the current climate. The box shows the range between the GCMs. Bottom: Same as middle, but for F2. This figure is available in colour online at wileyonlinelibrary.com/journal/joc

per grid cell, and second they were averaged to calculate the country average. Figure 7 shows scatter plots with the monthly change in precipitation and ETref for each of the 22 countries for F2 with respect to the current climate. The change is shown for the median of the nine GCMs. Water scarcity increases if the data points are located in the upper-left corner of the scatter plots, representing a decrease in precipitation and an increase in ETref. For most countries, the pressure on water availability becomes higher during March through May, and September. April through September are months with increased water demand (increase in ETref) for all countries. For June through August, the majority of countries is concentrated on the $x = 0$ axis, meaning limited change in precipitation, but a significant increase in ETref. In contrast to these months, November and

Copyright © 2013 Royal Meteorological Society

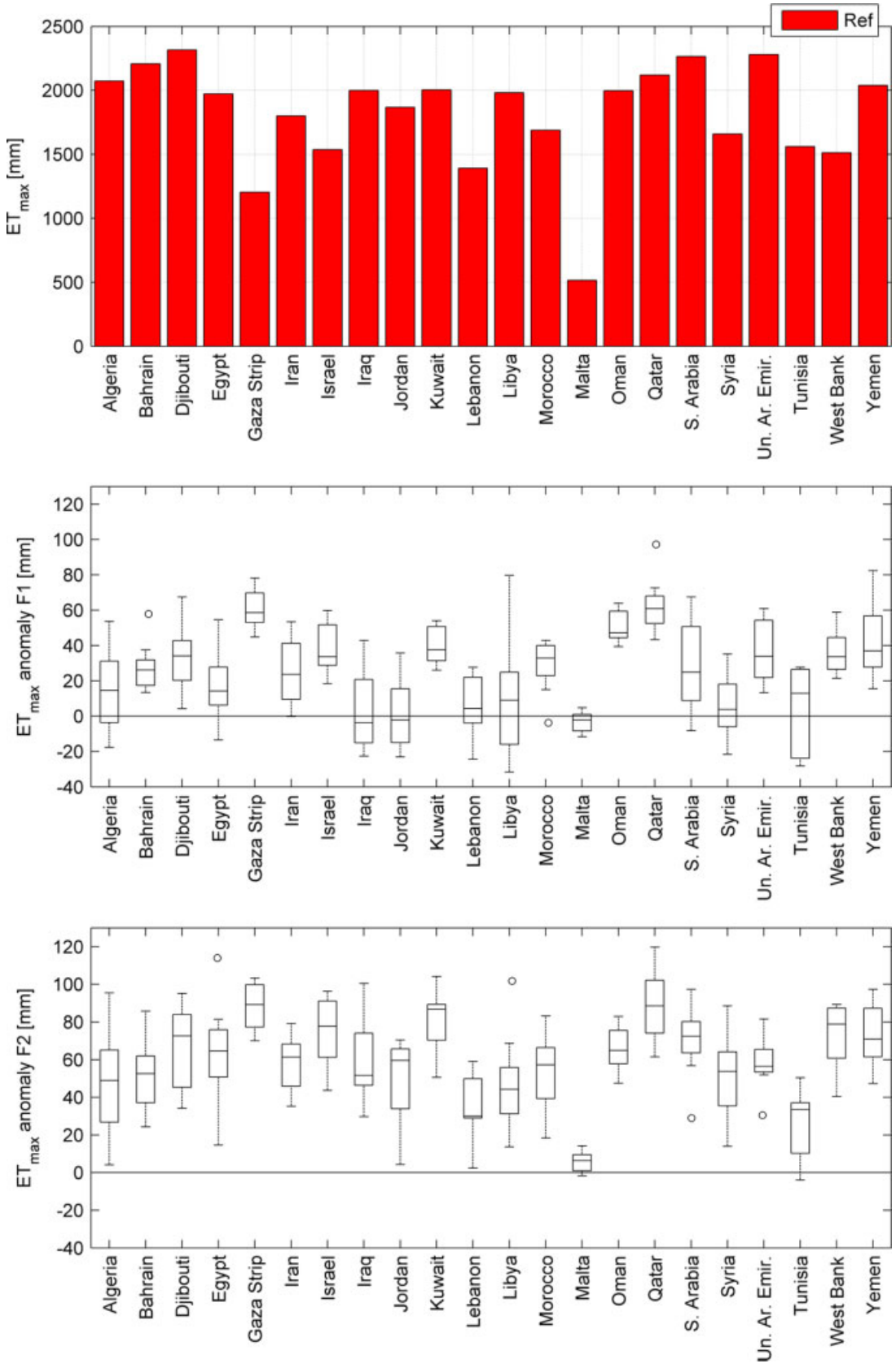

Figure 6. Top: Maximum annual ETref of the current climate for each of the 22 MENA countries. Middle: Boxplot of maximum annual ETref anomaly of F1 with respect to the current climate. The box shows the range between the GCMs. Bottom: Same as middle, but for F2. This figure is available in colour online at wileyonlinelibrary.com/journal/joc

Copyright © 2013 Royal Meteorological Society

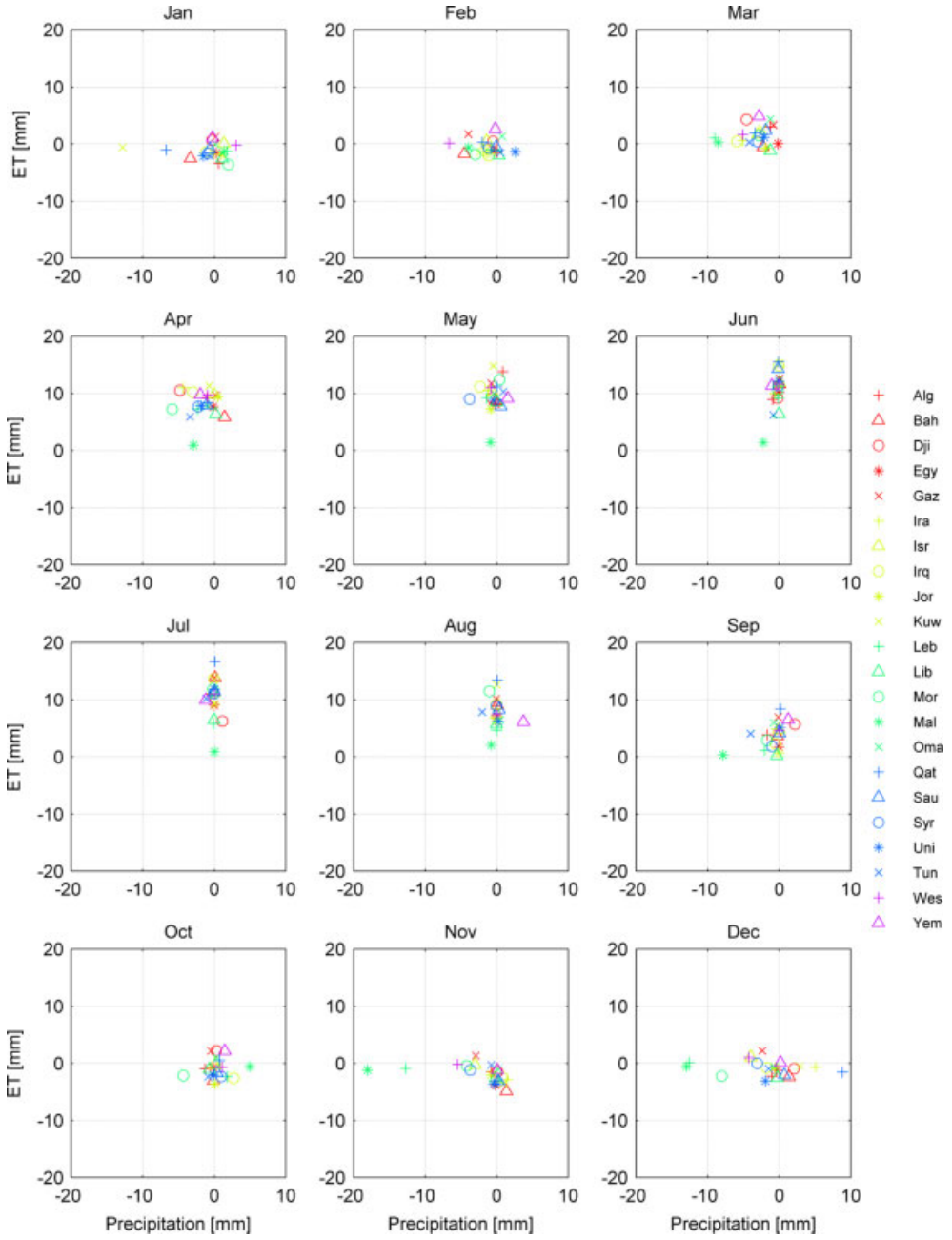

Figure 7. Monthly change in average precipitation and average ETref for F2 with respect to the current climate. The change is shown for the median of GCMs. This figure is available in colour online at wileyonlinelibrary.com/journal/joc

December show a relatively small change in ETref, but a significant change in precipitation, being a decrease for the majority of countries. Pressure on water availability seems to be most relevant for April.

3.5. Monthly extremes

For future adaptation strategies, the change in minimum precipitation and maximum ETref is more relevant than the change for the average situation (Figure 7). The monthly change in minimum precipitation and maximum ETref for F2 with respect to the current climate is shown in Figure 8. Apparently there is hardly any change in minimum precipitation. This same signal was found for the annual minimum precipitation. In contrast to this, the change in maximum ETref is quite significant. Especially April through August show a significant increase in ETref with increases up to 22 mm. Overall, it can be concluded that the maximum demand becomes higher during most months, while the minimum input (precipitation) does not become lower. Therefore, for the extreme situation, temperature is the most relevant climate variable.

3.6. Spatial analysis

The previous analyses were based on country averages. Climate change projections are likely to be spatially different within a country, especially in the larger ones. The spatial variability in climate change projections within a country has been analysed by calculating per grid cell,

Copyright © 2013 Royal Meteorological Society

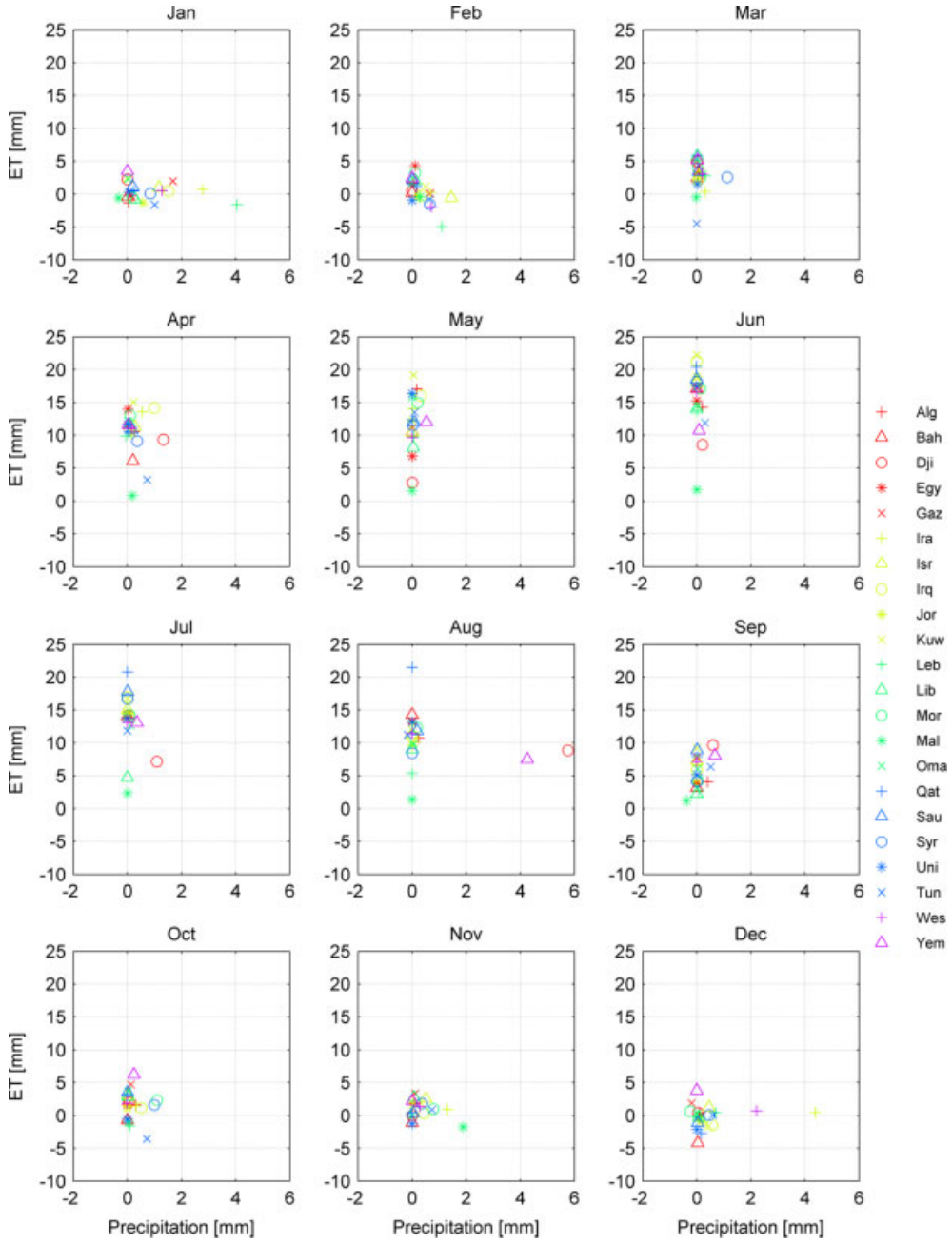

Figure 8. Monthly change in minimum precipitation and maximum ETref for F2 with respect to the current climate. The change is shown for the median of GCMs. This figure is available in colour online at wileyonlinelibrary.com/journal/joc

based on the average of the nine GCMs, (1) the average annual precipitation sum and ETref sum for the current climate, and (2) the anomalies of both precipitation and ETref for F1 and F2 with respect to the current climate. The results of this analysis are shown in Figure 9 for precipitation and in Figure 10 for ETref. It is clear that in the majority of countries the annual precipitation sum for the current climate is low. Especially in Libya and Egypt the annual precipitation sum is very small (<25 mm). The wetter areas are the coastal areas of Morocco, Algeria, Tunisia, Lebanon, Syria, Iran, and Yemen. Decreases in precipitation are nearly seen in every country for the period 2020–2030, with the largest decreases found in southern Egypt, Morocco, the central and coastal areas of Algeria, Tunisia, central Libya, Syria, and in the central and eastern part of Iran. Decreases are in the range of 5–15% for most countries, with a decrease of more than 20% in southern Egypt. In several regions, also increases in precipitation are noticed. Increases are in the range of 0–20%. It should be noted that the annual precipitation sum in these regions is very low, meaning that an increase of, for example, 20% in southeast Libya means an annual increase of roughly 5 mm. For 2040 through 2050 we see a larger decrease in precipitation for the majority of countries than for 2020 through 2030. Especially in Morocco, the central and northern part of Algeria, Tunisia, Syria,

Copyright © 2013 Royal Meteorological Society

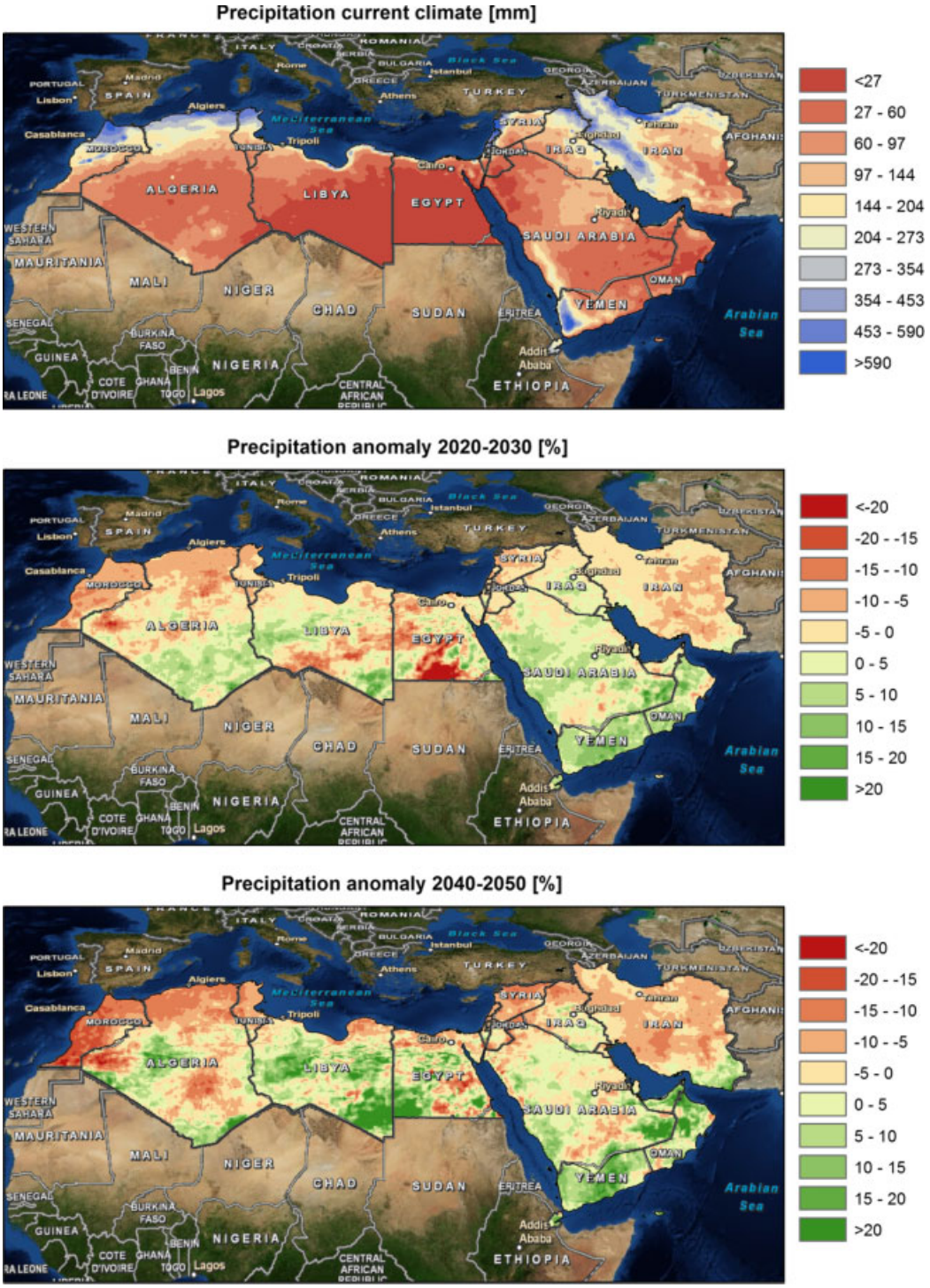

Figure 9. Spatial patterns of precipitation projections. Top: Average annual precipitation sum of the current climate. Middle: Precipitation anomalies of 2020–2030 with respect to the current climate. Bottom: Precipitation anomalies of 2040–2050 with respect to the current climate. This figure is available in colour online at wileyonlinelibrary.com/journal/joc

the southern and central part of Saudi Arabia, the northern part of Iraq, and in Iran, precipitation has decreased with respect to the current climate and 2020–2030.

A clear pattern of annual ETref can be observed for the current climate (Figure 10); coastal areas have the smallest annual ETref, while moving inland the ETref becomes higher. The largest annual ETref values (>2200 mm) are found in South Egypt, Djibouti, Southwest Algeria, the southern part of Iraq and Iran, the southeastern part of Saudi Arabia, Northeast Yemen, and West Oman. If we consider the anomalies for 2020–2030, then we notice a slight increase in annual ETref. This increase is in the range of 0–1% for the majority of the countries. However, as the current ETref is often in the range of 1000–2000 mm per year, the actual increase expressed in mm is substantial. Despite the lowest values of annual

Copyright © 2013 Royal Meteorological Society

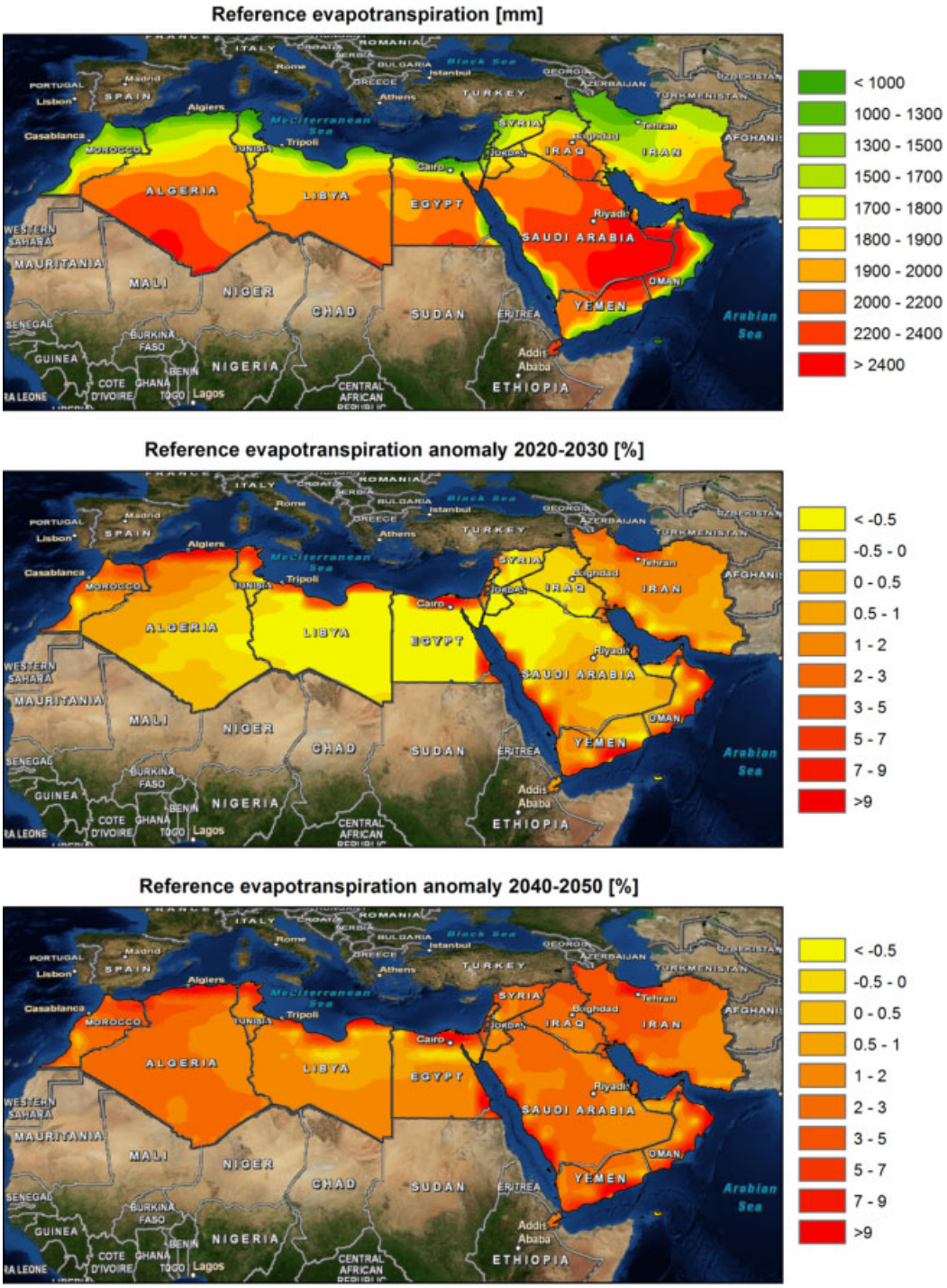

Figure 10. Spatial patterns of ETref projections. Top: Average annual ETref sum of the current climate. Middle: ETref anomalies of 2020–2030 with respect to the current climate. Bottom: ETref anomalies of 2040–2050 with respect to the current climate. This figure is available in colour online at wileyonlinelibrary.com/journal/joc

ETref found in the coastal areas, these areas are exposed to the largest (up to more than 9%) increase in annual ETref. In some countries, for example, in Algeria, Libya, Egypt, and Jordan, we see a small decrease in annual ETref. An increase in annual ETref can be noticed in all countries for 2040–2050, except for some small regions in Libya, Egypt, and Morocco. Again, these decreases are very small. The highest increases are again found in the coastal regions, with increases of more than 9%. Again, if we express this taken into account the actual value of ETref of 1500 mm, this 9% surpasses the change in expected precipitation substantially.

3.7. Morocco case study

Morocco was selected for a more in-depth country analysis because (1) agriculture is one of the major resources for a healthy Moroccan economy and is therefore highly relying on water, (2) it relies on its own national water

Copyright © 2013 Royal Meteorological Society

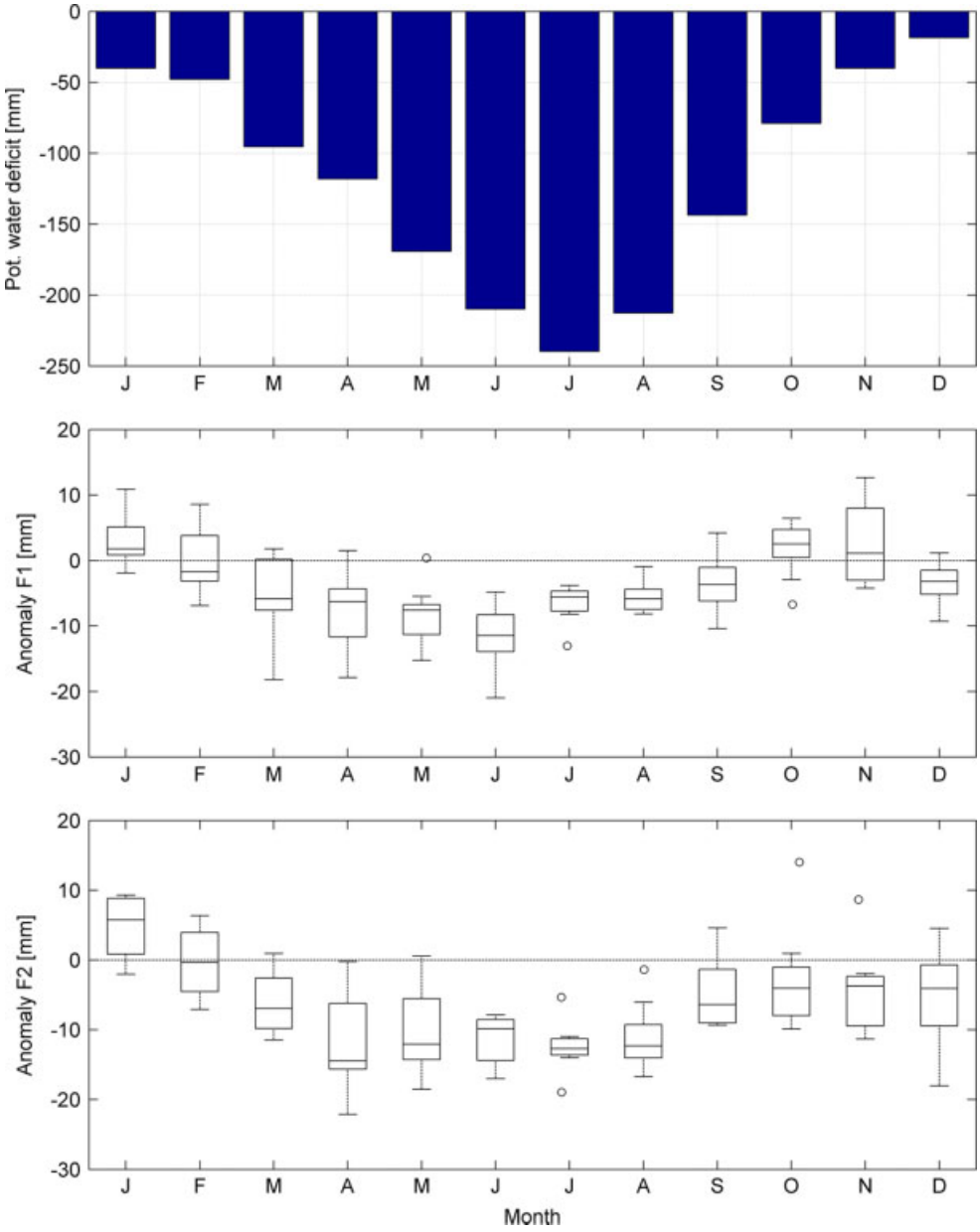

Figure 11. Top: Average monthly potential water deficit for the current climate for Morocco. Middle: Boxplot of average monthly water deficit anomaly of F1 with respect to the current climate. The box shows the range between the GCMs. Bottom: Same as middle, but for F2. This figure is available in colour online at wileyonlinelibrary.com/journal/joc

resources, (3) it shows a decrease in average annual precipitation combined with an increase in annual ETref for both F1 and F2, (4) the minimum annual precipitation sum decreases combined with an increase in maximum annual ETref for both F1 and F2, and (5) the within-country climate variability in space and time is significant. The combination of the projected population increase and the decrease in water availability put more pressure on effective water management strategies.

A well-known term is the potential water deficit, which is often defined as P-ETref. To evaluate the potential water deficit per crop it would be better to use P-Tp, whereas Tp is defined as the potential transpiration. This approach, however, requires a crop-specific crop factor. The actual transpiration, Ta, is defined as the amount of water a crop would transpire under a given amount of available water. If not enough water is available to meet the potential transpiration, then the actual transpiration will be lower than the potential transpiration, resulting in decreased crop yields. To study the effects of climate change on the potential and actual transpiration, advanced hydrological models are required, which is out of the scope of this study. For a quick-scan approach for Morocco, it is assumed that the overall country crop factor equals 1, meaning that we use the general approach P-ETref to assess the potential water deficit.

The potential water deficit in Morocco for each month for the current climate is shown in the top of Figure 11. The water deficit anomalies for F1 with respect to the current climate are shown in the middle of Figure 11,

Copyright © 2013 Royal Meteorological Society

whereas the bottom of Figure 11 represents the water deficit anomalies for F2 with respect to the current climate. The boxplots show the range in GCM anomalies. For the current climate Morocco already experiences a significantly large potential water deficit, which ranges from 20 mm in December up to 240 mm in July. Considering F1, we notice a potential water deficit increase during February through September, and December. For October, November, and January the water deficit becomes smaller. During F2 all months, except for January, show that the potential water deficit becomes larger. On the basis of these numbers, it is obvious that the Moroccan government will face huge challenges in managing their water resources in the future. Morocco has a couple of large reservoirs, e.g. the Al Wahda reservoir (Snoussi *et al.*, 2002), to store water for irrigation purposes and hydropower generation. On the basis of the increased potential water deficit in the future, it is therefore wise to store more water in the reservoirs in periods of excess rainfall, in order to have enough irrigation water during growing season.

4. Conclusions

The overall objective of this study was to undertake a climate change assessment for the MENA countries by analysing the change in precipitation (supply) and ETref (demand) in order to stress the problems these countries may encounter around 2050. Two future periods, defined as F1 (2020–2030) and F2 (2040–2050), were compared with a current climate (2000–2009). Overall, conclusions that are in line with what others (e.g. Christensen *et al.* (2007)) have found are as follows:

1 Average annual precipitation decreases for F1 and F2 for the majority of countries, with the largest decreases found for F2 (15–20%).
2 Some countries in the southeastern part of MENA, e.g. Djibouti and Yemen, showed an increase in average annual precipitation for F1 and F2 (15–20%).
3 An overall increase in average annual ETref was found for both F1 and F2, with the largest increases found for F2.

The results are quite different for the eastern part of MENA. Both Christensen *et al.* (2007) and this study project an increase in precipitation of 15–20%, e.g. Djibouti and Yemen, whereas our study focuses on 2040–2050, and Christensen *et al.* (2007) focuses on 2080–2099. A possible explanation could be that the precipitation signal remains more or less constant after 2050 for this part of MENA. This is as such not further investigated and out of the scope of this study. It is, however, recommended to investigate the change in precipitation signal for this part of Africa in a future study.

It would be preferred to compare our ETref projections with ETref projections from another study. Unfortunately, until recently no other study was found in which ETref projections were made for the 21st century. It is important to realize that the ETref can be translated into the real demand for water, while the water that really evaporates (actual evapotranspiration) also depends on the water availability. A study by Jung *et al.* (2010) showed that a recent decline in the global evapotranspiration trend, particularly in Africa and Australia, is due to limited soil moisture supply. Therefore, the increase in ETref as found in this study is a result of climate change, whereas the actual evapotranspiration is a result of both climate change and land–water interactions.

A striking result from this study is that while for the extreme situation the maximum annual ETref increases, the minimum annual precipitation does not decrease. In contrast, the minimum annual precipitation increases. Besides annual values, this also holds for monthly values. A similar result was found by Shongwe *et al.* (2011) for East Africa. The fact that the minimum annual and minimum monthly precipitation do not decrease for the future climate indicates that the focus for the extreme situation should be more on demand driven (ETref) than on supply driven (precipitation). However, care should be taken when interpreting these results. There may be a signal that indicates that the climate becomes more extreme in the sense of 'dryness'. Despite the fact that the minimum monthly and minimum annual precipitation sums do not become smaller, the drier signal may be hidden in another variable such as the number of dry days. It is not unlikely that the number of dry days increases for the future climate. This is as such not further investigated in this study, but is recommended as follow-up for future studies.

Monthly analysis showed that pressure on water availability for the majority of countries increases during March through May, and September. For June through August it was shown that the water demand (increased ET) plays a larger role than water availability (precipitation). The opposite is true for November to December, with a relatively small change in water demand, but a larger change in water availability.

Spatial analysis showed precipitation decreases (5–15%) in nearly every country, with southern Egypt, Morocco, the central and coastal areas of Algeria, Tunisia, central Libya, Syria, and the central and eastern part of Iran showing the largest decreases. A clear pattern with lower ET values was noticed along the coastal areas with higher values more inland. Because of the climate change an overall increase in ET is noticed, with increases up to 9% in the coastal areas. Some countries, however, e.g. Djibouti and Malta, are very small compared with countries, e.g. Algeria. Because the size of these countries is very small, they are only covered within one GCM grid cell. This means that the statistical downscaling of GCM data to a resolution of 10 km involves GCM grid cells outside the country. Therefore, the country data are highly affected by GCM data outside the country GCM grid cell data. This can be translated into a higher uncertainty in climate projections for small countries that cover only one or two GCM grid cells.

Besides the strength of this study, there are some drawbacks to be discussed. The main uncertainties in this

Copyright © 2013 Royal Meteorological Society

climate impact study, among other climate studies, are the GCMs used in climate studies. A major issue with GCMs is that vegetation feedbacks and feedbacks from dust aerosol production are not included in the global models (Hulme *et al.*, 2001; Christensen *et al.*, 2007). Also, possible future land surface modifications are not taken into account in GCM projections. This incorporates a certain amount of error in the GCM projections, which will further accumulate when downscaling to a smaller resolution. Therefore, an interesting follow-up would be to evaluate the impacts of land use change in combination with climate change on water availability in MENA in the future. This would also involve improving GCMs by the implementation of vegetation feedbacks.

This study uses climate data of the CMIP3 multi-model ensemble. Currently, new emission scenarios (CMIP5 multi-model ensemble) (Hibbard *et al.*, 2007; Meehl and Hibbard, 2007; Meehl *et al.*, 2009; WCRP, 2011; Taylor *et al.*, 2012) are available. These scenarios are not used in this study, because the focus of this study is exclusively on climate data from the CMIP3 model ensemble because it includes the full bandwidth of possible future climates. Moreover, the complete CMIP5 model ensemble was unavailable at the time of the study and this would introduce a possible bias in our results. Finally, the new approach adopted for AR5 based on RCPs is just a slight improvement from the SRES approach used for AR4. A systematic comparison between CMIP3 and CMIP5 models and the SRES and RCP approaches would however definitely be recommendable for a future study.

It is well known that the change in surface variables can be related to the behaviour of large-scale circulations, e.g. ENSO (El Niño – Southern Oscillation) (Palmer *et al.*, 1992; Ward, 1992; Fontaine *et al.*, 1995, 1998; Janicot *et al.*, 1998; Neelin *et al.*, 1998) and the African Easterly Jet (Parker *et al.*, 2005, 2008; Redelsperger *et al.*, 2006; Dezfuli and Nicholson, 2010). According to Yeshanew and Jury (2007), the Sahelian climate of Northern Africa is characterized by a decadal rhythm, whereas the mountainous eastern and equatorial regions of Africa exhibit interannual cycles. Yeshanew and Jury (2007) also found that ENSO-modulated zonal circulations over the Atlantic Pacific sector are important for decadal variations, and that they create a climatic polarity between South America and tropical North Africa. It is likely that climate change will have repercussions on large-scale circulation patterns, which may consequently influence Africa's climate. This assessment is far beyond the scope of this study, but it is recommended to focus future research on this topic.

For policy makers it is relevant to know how much water is available currently and in the future, and what adaption strategies are available at what cost to overcome the possible projected water shortage. Therefore, two beneficial studies are required:

- A study that addresses water availability using a hydrological model (Immerzeel *et al.*, 2012); this involves relevant hydrological processes, e.g. inflow from upstream basins, reservoir storage, irrigation water supply, and routing of streamflow, which are not incorporated in this study.
- A study that evaluates adaption strategies and their implementation costs in order to overcome possible water shortages in the future (Droogers *et al.*, 2012).

References

Allen R, Pereira L. 1998. Crop evapotranspiration. Guidelines for computing crop water requirements. *FAO Irrigation and Drainage Paper* 56.

Anyah R, Semazzi F. 2007. Variability of East African rainfall based on multiyear RegCM3 simulations. *International Journal of Climatology* **27**: 357–371. DOI: 10.1002/joc.1401.

Arnell N, Hudson D, Jones R. 2003. Climate change scenarios from a regional climate model: estimating change in runoff in southern Africa. *Journal of Geophysical Research* **108**: 4519. DOI: 10.1029/2002JD002782.

Christensen J, Hewitson B, Busuioc A, Chen A, Gao X, Held I, Jones R, Kolli R, Kwon WT, Laprise R, Rueda VM, Mearns L, Menéndez C, Räisänen J, Rinke A, Sarr A, Whetton P. 2007. Regional Climate Projections. In *Climate Change 2007: The Physical Science Basis. Contribution of Working Group I to the Fourth Assessment Report of the Intergovernmental Panel on Climate Change*, Solomon S, Qin D, Manning M, Chen Z, Marquis M, Averyt KB, Tignor M, Miller HL (eds). Cambridge University Press: Cambridge, United Kingdom and New York, NY.

Dezfuli AK, Nicholson SE. 2010. A note on long-term variations of the African easterly jet. *International Journal of Climatology* **31**(13): 2049–2054. DOI: 10.1002/joc.2209.

Droogers P, Allen R. 2002. Estimating reference evapotranspiration under inaccurate data conditions. *Irrigation and Drainage Systems* **16**(1): 33–45. DOI: 10.1023/A:1015508322413.

Droogers P, Immerzeel WW, Terink W, Hoogeveen J, Bierkens M, van Beek R, Debele B. 2012. Water resources trends in Middle East and North Africa towards 2050. *Hydrology and Earth System Sciences* **16**: 1–14. DOI: 10.5194/hess-16-1-2012.

Fontaine B, Janicot S, Moron V. 1995. Rainfall anomaly patterns and wind field signals over West Africa in August (1958–1989). *Journal of Climate* **8**: 1503–1510.

Fontaine B, Trzaska I, Janicot S. 1998. Evolution of the relationship between near global and Atlantic SST mode and the rainy season in West Africa: statistical analyses and sensitivity experiments. *Climate Dynamics* **14**: 353–368.

Giorgi F, Francisco R. 2000a. Evaluating uncertainties in the prediction of regional climate change. *Geophysical Research Letters* **27**(9): 1295–1298. DOI: 10.1029/1999GL011016.

Giorgi F, Francisco R. 2000b. Uncertainties in regional climate change prediction: a regional analysis of ensemble simulations with the HADCM2 coupled AOGCM. *Climate Dynamics* **16**(2–3): 169–182. DOI: 10.1029/1999GL011016.

Giorgi F, Mearns L. 1991. Approaches to the simulation of regional climate change: a review. *Reviews of Geophysics* **29**(2): 191–216. DOI: 10.1029/90RG02636.

Hargreaves G, Samini Z. 1985. Reference crop evapotranspiration from temperature. *Applied Engineering in Agriculture* **1**(2): 96–99.

Haylock R, Cawley G, Harpham C, Wilby R, Goodess C. 2006. Downscaling heavy precipitation over the United Kingdom: a comparison of dynamical and statistical methods and their future scenarios. *International Journal of Climatology* **26**(10): 1397–1415. DOI: 10.1002/joc.1318.

Hewitson B, Crane R. 1996. Climate downscaling: techniques and application. *Climate Research* **7**: 85–95. DOI: 10.3354/cr0007085.

Hibbard KA, Meehl GA, Cox P, Friedlingstein P. 2007. A strategy for climate change stabilization experiments. *Eos* **88**: 217. DOI: 10.1029/2007EO200002.

Hulme M, Doherty R, Ngara T, New M, Lister D. 2001. African climate change: 1900–2100. *Climate Research* **17**: 145–168.

Hurkmans R, Terink W, Uijlenhoet R, Torfs P, Jacob D, Troch PA. 2010. Changes in streamflow dynamics in the Rhine Basin under three high-resolution regional climate scenarios. *Journal of Climate* **23**: 679–699. DOI: 10.1175/2009JCLI3066.1.

Copyright © 2013 Royal Meteorological Society

Immerzeel WW. 2008. Historical trends and future predictions of climate variability in the Brahmaputra basin. *International Journal of Climatology* **28**: 243–254. DOI: 10.1002/joc.1528.

Immerzeel WW, Droogers P, Terink W, van Beek R, Bierkens MFP. 2012. *Water Resources Management*.

IPCC. 2007. Climate Change 2007: Synthesis Report. IPCC 2007. Technical report, IPCC.

Janicot S, Harxallah A, Fontaine B, Moron V. 1998. WestAfrican monsoon dynamic and eastern equatorial Atlantic and Pacific SST anomalies (1970–1988). *Journal of Climate* **11**: 1874–1882.

Jung M, Reichstein M, Ciais P, Seneviratne S, Sheffield J, Goulden M, Bonan G, Cescatti A, Chen J, de Jeu R, Dolman A, Eugster W, Gerten D, Gianelle D, Gobron N, Heinke J, Kimball J, Law B, Montagnani L, Mu Q, Mueller B, Oleson K, Papale D, Richardson A, Roupsard O. 2010. Recent decline in the global land evapotranspiration trend due to limited moisture supply. *Nature* **467**: 951–954.

Kalnay E, Kanamitsu M, Kistler R, Collins W, Deaven D, Gandin L, Iredell M, Saha S, White G, Woollen J, Zhu Y, Chelliah M, Ebisuzaki W, Higgins W, Janowiak J, Mo K, Wang JCR, Leetmaa A, Reynolds R, Jenne R, Joseph D. 1996. The NCEP/NCAR 40-year reanalysis project. *Bulletin of the American Meteorological Society* **77**: 437–470.

Kidson J, Thompson C. 1998. A comparison of statistical and model-based downscaling techniques for estimating local climate variations. *Journal of Climate* **11**(4): 735–753. http://dx.doi.org/10.1175/1520-0442(1998)011<0735:ACOSAM>2.0.CO;2.

Kummerow C, Simpson J, Thiele O, Barnes W, Chang A, Stocker E, Adler R, Hou A, Kakar R, Wentz F, Ashcroft P, Kozu T, Hong Y, Iguchi KOT, Kuroiwa H, Im E, Haddad Z, Huffman G, Ferrier B, Olson W, Zipser E, Smith E, Wilheit T, North G, Krishnamurti T, Nakamur K. 2000. The status of the Tropical Rainfall Measuring Mission (TRMM) after two years in orbit. *Journal of Applied Meteorology* **39**(12): 1965–1982. DOI: 10.1175/1520-0450(2001)040<1965:TSOTTR>2.0.CO;2.

Meehl GA, Hibbard KA. 2007. A strategy for climate change stabilization experiments with AOGCMs and ESMs. WCRP Informal Report No. 3/2007, ICPO Publication No. 112, IGBP Report No. 57. World Climate Research Programme: Geneva, 35pp.

Meehl GA, Goddard L, Murphy J, Stouffer RJ, Boer G, Danabasoglu G, Dixon K, Giorgetta MA, Greene AM, Hawkins E, Hegerl G, Karoly D, Keenlyside N, Kimoto M, Kirtman B, Navarra A, Pulwarty R, Smith D, Stammer D, Stockdale T. 2009. Decadal prediction. *Bulletin of the American Meteorological Society* **90**: 1467–1485. DOI: 10.1175/2009BAMS2778.1.

Mitasova H, Mitas L. 1993. Interpolation by regularized spline with tension: I. Theory and implementation. *Mathematical Geology* **25**(6): 641–655. DOI: 10.1007/BF00893171.

Murphy J. 1999. An evaluation of statistical and dynamical techniques for downscaling local climate. *Journal of Climate* **12**(8): 2556–2284. http://dx.doi.org/10.1175/1520-0442(1999)012<2256:AEOSAD>2.0.CO;2.

Neelin JD, Battisti DS, Hirst AC, Jin FF, Wakata Y, Yamagata T, Zebiak SE. 1998. ENSO theory. *Journal of Geophysical Research* **103**(C7): 14261–14290.

New M, Hulme M, Jones P. 2000. Representing twentieth-century space-time climate variability. Part II: Development of 1901–96 monthly grids of terrestrial surface climate. *Journal of Climate* **13**(13): 2217–2238. http://dx.doi.org/10.1175/1520-0442(2000)013<2217:RTCSTC>2.0.CO;2.

Paeth H, Hense A. 2004. SST versus climate change signals in West African rainfall: 20th-century variations and future projections. *Climatic Change* **65**(1–2): 179–208. DOI: 10.1023/B:CLIM.0000037508.88115.8a.

Palmer TN, Brankovic C, Viterbo P, Miller MJ. 1992. Modeling the interannual variation of summer monsoon. *Journal of Climate* **5**: 299–417.

Parker DJ, Thorncroft CD, Burton RR, Diongue-Niang A. 2005. Analysis of the African easterly jet using aircraft observations from the JET2000 experiment. *Quarterly Journal of the Royal Meteorological Society* **131**(608): 1461–1482.

Parker DJ, Fink A, Janicot S, Ngamini JB, Douglas M, Afiesimama E, Agusti-Panareda A, Beljaars A, Did'e F, Diedhiou A, Lebel T, Polcher J, Redelsperger JL, Thorncroft CD, Wilson GA. 2008. The AMMA radiosonde program and its implications for the future of atmospheric monitoring over Africa. *Bulletin of the American Meteorological Society* **89**: 1015–1027.

Redelsperger JL, Thorncroft CD, Diedhiou A, Lebel T, Parker DJ, Polcher J. 2006. African Monsoon Multidisciplinary Analysis (AMMA): an international research project and field campaign. *Bulletin of the American Meteorological Society* **87**: 1739–1746.

Roudi-Fahimi F, Kent M. 2007. Challenges and opportunities – the population of the Middle East and North Africa. *Population Bulletin* **62**(2): 5.

Shongwe M, van Oldenborgh G, van den Hurk B, de Boer B, Coelho C, van Aalst M. 2009. Projected changes in mean and extreme precipitation in Africa under global warming. Part I: Southern Africa. *Journal of Climate* **22**: 3819–3837. 10.1175/2009JCLI2317.1.

Shongwe M, van Oldenborgh G, van den Hurk B, van Aalst M. 2011. Projected changes in mean and extreme precipitation in Africa under global warming, Part II: East Africa. *Journal of Climate* **24**(11): 3718–3733. DOI: http://dx.doi.org/10.1175/2010JCLI2883.1.

Snoussi M, Haṙda S, Imassi S. 2002. Effects of the construction of dams on the water and sediment fluxes of the Moulouya and the Sebou Rivers, Morocco. *Regional Environmental Change* **3**(1–3): 5–12. DOI: 10.1007/s10113-001-0035-7.

Snyder JP. 1987. Map Projections – A Working Manual. *U.S. Geological Survey Professional Paper* 1395. U.S. Government Printing Office: Washington, DC, 98–103.

SRES. 2000. IPCC Special Report Emission Scenarios. Summary for Policy makers. Intergovernmental Panel on Climate Change. ISBN: 92-9169-113-5.

Taylor KE, Stouffer RJ, Meehl GA. 2012. An Overview of CMIP5 and the experiment design. *Bulletin of the American Meteorological Society* **93**: 485–498. DOI: 10.1175/BAMS-D-11-00094.1.

Terink W, Hurkmans RTWL, Torfs PJJF, Uijlenhoet R. 2010. Evaluation of a bias correction method applied to downscaled precipitation and temperature reanalysis data for the Rhine basin. *Hydrological and Earth System Sciences* **14**: 687–703.

Van Beek LPH, Bierkens MFP. 2009. The global hydrological model PCR-GLOBWB: conceptualization, parameterization and verification. Report, Department of Physical Geography, Utrecht University, Utrecht, The Netherlands, http://vanbeek.geo.uu.nl/suppinfo/vanbeekbierkens2009.pdf.

Ward MN. 1992. Worldwide ocean-atmosphere surface fields and Sahelian rainfall variability. *Journal of Climate* **5**: 454–475.

WCRP. 2011. WCRP Coupled Model Intercomparison Project – Phase 5 – CMIP5. *CLIVAR Exchanges. Special issue*. 16(2).

Wilby R, Wigley T. 1997. Downscaling general circulation model output: a review of methods and limitations. *Progress in Physical Geography* **21**(4): 530–548. DOI: 10.1177/030913339702100403.

Wilby R, Wigley T, Conway D, Jones P, Hewitson B, Main J, Wilks D. 1998. Statistical downscaling of general circulation model output: a comparison of methods. *Water Resources Research* **34**(11): 2995–3008.

Wilby R, Hay L, Gutowski W Jr, Arrit R, Takle E, Pan Z, Leavesley G, Clark M. 2000. Hydrological responses to dynamically and statistically downscaled climate model output. *Geophysical Research Letter* **27**(8): 1199–1202.

Wilby R, Dawson C, Barrow E. 2002. SDSM – a decision support tool for the assessment of regional climate change impacts. *Environmental Modelling & Software* **17**(2): 147–159. DOI: http://dx.doi.org/10.1016/S1364-8152(01)00060-3.

World Bank. 2007. Making the most of scarcity. Accountability for better water management results in the Middle East and North Africa. MENA Development Report, World Bank. DOI: 10.1596/978-0-8213-6925-8.

Yeshanew A, Jury MR. 2007. North African climate variability. Part 2: Tropical circulation systems. *Theoretical and Applied Climatology* **89**: 37–49.

Zwiers F, Kharin V. 1997. Changes in the extremes of the climate simulated by CCC GCM2 under CO_2 doubling. *Journal of Climate* **11**(9): 2200–2222. http://dx.doi.org/10.1175/1520-0442(1998)011<2200:CITEOT>2.0.CO;2.

Copyright © 2013 Royal Meteorological Society